## Journal of the Air & Waste Management Association

# Use of Two Different Acidic Aerosol Samplers To Measure Acidic Aerosols in Hsinchu, Taiwan

Chuen-Jinn Tsai [a] , Shie-Bong Perng [a] & Shin-Fu Chiou [a]

[a] Institute of Environmental Engineering, National Chiao Tung University , Hsinchu , Taiwan
Published online: 27 Dec 2011.

PLEASE SCROLL DOWN FOR ARTICLE

# Use of Two Different Acidic Aerosol Samplers To Measure Acidic Aerosols in Hsinchu, Taiwan

**Chuen-Jinn Tsai, Shie-Bong Perng, and Shin-Fu Chiou**
*Institute of Environmental Engineering, National Chiao Tung University, Hsinchu, Taiwan*

## ABSTRACT

Acidic aerosol concentrations measured by an annular denuder system (ADS) and a honeycomb denuder system (HDS) in Hsinchu, Taiwan, were compared. Aerosols were also sampled by a MOUDI (micro-orifice uniform deposit impactor) and analyzed by an ion chromatograph to determine the size distributions of different species. Using the measured aerosol size distribution, theoretical analysis showed that positive $HNO_3$ artifact due to volatilization of $NH_4NO_3$ is generally negligible for both samplers. Comparing two different denuder samplers, the average concentration of $HNO_3$ measured by the ADS was found to be lower than that measured by the HDS, while the difference between the two samplers for the average concentration of other species was found to be within ±15%. A possible cause of the difference in $HNO_3$ concentrations is due to a greater loss of $HNO_3$ in the cyclone used by the ADS than in the impactor used by the HDS. The study also showed incomplete absorption of the evaporated HCl and $HNO_3$ from the particles on the Teflon filter by the first nylon filter in the filter pack of the ADS. Collection efficiency and capacity of HCl and $HNO_3$ by the nylon filters need further investigation.

## INTRODUCTION

Acidic air pollutants have been associated with adverse health effects, mainly respiratory diseases. Spengler et al.

---

**IMPLICATIONS**

Measured concentrations of two commonly used acidic aerosol samplers—ADS and HDS—were compared in Hsinchu. Theoretical analysis showed that positive $HNO_3$ artifact due to volatilization of $NH_4NO_3$ is generally negligible for both samplers. Experimental results showed that agreement between the measured acidic aerosol concentration is good, except for species which have a low concentration, such as $HNO_3$. A possible cause of the difference in $HNO_3$ concentration is due to a greater loss of $HNO_3$ in the cyclone used by the ADS than in the impactor used by the HDS, leading to consistently higher $HNO_3$ concentrations measured by the HDS.

---

reviewed extensively the health effect, health evidence, concentration ranges, and epidemiologic studies of acidic aerosols.[1] Concentration ranges of $SO_4^{2-}$ and $H^+$ in selected North American cities were shown to depend on sampling location and time of year. For example, in a 9-month study, from December 1985 to September 1986, the mean $H^+$ concentrations in Kingston, TN, and St. Louis, MO, were found to be 36.1 and 10.3 $nmol/m^3$, respectively.[2] The reason that acidity for Kingston was much higher than that for St. Louis is because the latter is more urban, and more aerosol neutralization by $NH_3$ occurred.

Many different acidic aerosol samplers are commercially available. Possanzini et al. designed an annular denuder/filter pack system (ADS) that collects reactive atmospheric pollutants more efficiently per unit length than does a tubular denuder.[3] An alternative system called the honeycomb denuder system (HDS) was developed by Koutrakis et al.[4] and improved by Sioutas et al.,[5] whose field studies indicated an excellent agreement between the HDS and HEADS (Harvard-EPA Annular Denuder System) for determining the concentrations of particulate $SO_4^{2-}$, $NH_4^+$, $H^+$, and gas-phase $HNO_3$ and $NH_3$.

In this study, we used an ADS (University Research Glassware Inc.) and an HDS (Ogawa & Co. Inc.) to compare the performance of these two different systems. During the experiment, a 10-stage micro-orifice uniform deposit impactor (MOUDI) was collocated with the two denuder samplers to measure the size distributions of acidic aerosols in the atmosphere. The gas collection section of the HDS is a glass honeycomb consisting of 212 cylindrical tubes, and the i.d. and length of each tube are 0.2 and 3.8 cm, respectively.[4,5] The gas collection section of the ADS consists of 3 annuli, and the o.d. and i.d. are 19 and 17 mm, 14 and 12 mm, and 10 and 8 mm for the first, second, and third annuli, respectively, according to the manufacturer. The total flow rate and residence time, 10 L/min and 0.15 sec, are the same for both denuders.

In the following section, theoretical analysis will be presented to show if the positive $HNO_3$ is severe for both denuder samplers. Experimental methods and results will follow.

## THEORETICAL ANALYSIS OF EVAPORATION LOSS OF $NH_4NO_3$ PARTICLES IN DENUDERS

For evaporative particulate species, such as $NH_4NO_3$ or $NH_4Cl$, positive $HNO_3$ artifact is formed due to particle evaporation. Bai et al.[6] proposed a numerical method to calculate the amount of such artifact, and an analytical method is proposed here. Only $NH_4NO_3$ particle is considered. Gas penetration (or 1.0 – gas collection efficiency) of the HDS can be calculated as[7]

$$P = 1 - 5.5\mu^{2/3} + 3.77\mu, \, for \, \mu < 0.009$$
$$P = 0.819\exp(-11.5\mu) + 0.0975\exp(-70.1\mu), \, for \, \mu \geq 0.009 \quad (1)$$

where $\mu = DL/Q$, $L$ is the length of the tube, $D$ is the diffusivity of a gas or particle, and $Q$ is the flow rate through each tube. Similarly, the gas penetration of the ADS can be calculated as[7]

$$P = 1.0 - 2.96\mu^{2/3} + 0.4\mu, \, for \, \mu < 0.005$$
$$P = 0.91\exp(-7.54\mu) + 0.0531\exp(-85.7\mu), \, for \, \mu \geq 0.005 \quad (2)$$

where $\mu = \pi DL(\text{o.d.} + \text{i.d.})/[Q(\text{o.d.} - \text{i.d.})]$, and $Q$ is the flow rate through each annular space.

Figure 1 compares the penetration of $HNO_3$ gas and a 0.01-$\mu$m particle at the different dimensionless lengths, $x/L$, of the two denuders. Diffusivity of $HNO_3$ is 0.118 $cm^2/sec$ at normal temperature and pressure.[8] As can be seen, $HNO_3$ is depleted very quickly in both denuders. More than 80% of the nitric gas is absorbed in the first 7 or 20% of the length of the ADS or HDS, respectively. In comparison, particle diffusion loss is almost negligible due to much smaller diffusivity of particles compared with that of gases. For small 0.01-$\mu$m particles, the loss is only ~10% over the entire length of both denuders. Therefore, when calculating the evaporative loss of $NH_4NO_3$ particles, it is possible to assume that evaporated $HNO_3$ gas is absorbed immediately to the denuder tubes (or annuli), resulting in positive $HNO_3$ artifact, while the contribution of particle diffusion to $HNO_3$ artifact can be neglected.

To calculate evaporation loss of $NH_4NO_3$, the method described in Seinfeld and Pandis can be used.[9] Mass transfer flux, $J$ (in g/sec), from a particle can be calculated as

$$J = J_c \frac{0.75\alpha(1+K_n)}{K_n^2 + K_n + 0.283K_n\alpha + 0.75\alpha} \quad (3)$$

where $\alpha$ is the accommodation coefficient of a gas species, $K_n$ is the Knudsen number of the particle [$K_n$ is defined as $\lambda/(D_p/2)$, with $\lambda$ the mean free path of gas molecules, and $D_p$ the diam of the particle], and $J_c$ is the mass transfer flux in the continuum regime, which can be calculated as

$$J_c = 2\pi D_p D_g(C_\infty - C_s) \quad (4)$$

where $C_\infty$ and $C_s$ are $HNO_3$ acid concentrations in the air and over the particle surface, respectively. Since $HNO_3$ is absorbed very quickly in the denuders, $C_\infty$ can be treated as zero. $C_s$ can be calculated from the partial pressure of $HNO_3$, $P_{HNO_3}$, which is determined from the dissociation constant of $NH_4NO_3$ particles, $K_p$ (in $ppb^2$, defined as the product of and, the partial pressure of $NH_3$). The relationship of $K_p$ and ambient temperature $T$ (in K) for dry $NH_4NO_3$ particles is[10]

$$\ln K_p = 84.6 - \frac{24220}{T} - 6.1\ln(\frac{T}{298}) \quad (5)$$

Another formula, given by Mozurkewich,[11] is

$$\ln K_p = 118.87 - \frac{20484}{T} - 6.025\ln(T) \quad (6)$$

For particles in lognormal distribution, the total positive $HNO_3$ artifact can be integrated from eq 3 over the entire particle distribution once the particle mass median aerodynamic diameter (MMAD) and geometric standard deviation ($\sigma_g$) are known. In this study, the particulate $NO_3^-$ measured is assumed to be entirely $NH_4NO_3$, and only evaporation loss in the fine particle mode is calculated, since coarse particles are removed by the impactor or cyclone. The fine fraction of particulate $NO_3^-$ averages 71% of the total $NO_3^-$ concentration, as found in this study.

Both denuders have the same $HNO_3$ artifact concentration since the airflow residence time is the same (0.15 sec). Theoretical predictions of positive $HNO_3$ artifact are shown in Figures 2 and 3 using actual $NO_3^-$ concentrations
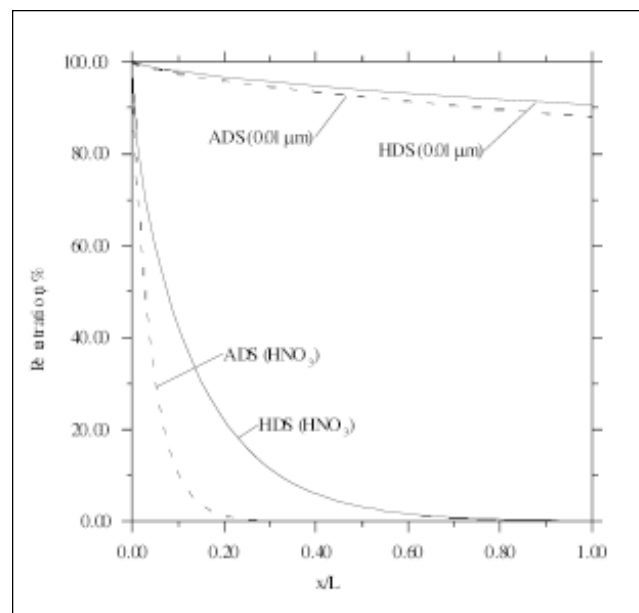


**Figure 1.** Gas or particle penetration of the ADS and HDS vs. dimensionless length.
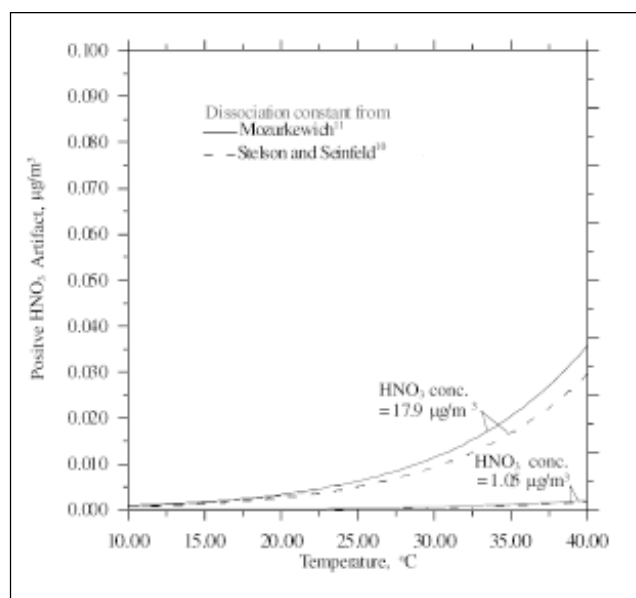
**Figure 2.** Positive $HNO_3$ artifact vs. ambient temperature assuming two different particulate $NO_3$ concentrations. MMAD and $s_g$ are assumed to be 0.5 µm and 1.5, respectively.



**Figure 3.** Positive $HNO_3$ artifact vs. ambient temperature assuming different particle size distributions in the fine mode. Particulate $NO_3$ concentration is assumed to be 17.9 µg/m³, and dissociation constant is calculated from Mozurkewich.[11]

and particle size distributions measured in this study. The accommodation coefficient of 0.52 is adopted.[12] In Figure 2, the MMAD and $s_g$ in the fine mode are assumed to be 0.5 µm and 1.5, respectively. The $HNO_3$ artifact is shown to be small and increases with increasing ambient temperature and particulate $NO_3^-$ concentration. The dissociation constant determined by Mozurkewich[11] gives a slightly higher $HNO_3$ artifact concentration than that given by Stelson and Seinfeld.[10] The maximum concentration is only 0.038 µg/m³ at 40 °C when the $NO_3^-$ concentration is 17.9 µg/m³, which is the maximum $NO_3^-$ concentration found in this study.

Size distribution of particulate $NO_3^-$ influences the $HNO_3$ artifact concentration for a given particle $NO_3^-$ concentration, 17.9 µg/m³ (see Figure 3). It is seen that a smaller MMAD and larger $\sigma_g$ results in a higher artifact concentration. However, the artifact $HNO_3$ concentration is still small. In this study, the ambient temperature averaged 28 °C and the $HNO_3$ concentration averaged 0.6 µg/m³; hence, it can be said that $HNO_3$ artifact due to evaporation loss of $NO_3^-$ particles is not a problem for either denuder.

**EXPERIMENTAL METHODS**
A total of 15 ambient 24-hr-average samples were collected from December 1997 to May 1998 on the roof of the Institute of Environmental Engineering, National Chiao Tung University (~11 m above ground level), located in Hsinchu, Taiwan. Due to frequent rain in the winter season, 11 of the 15 samples were collected in the spring season (March–May). The city has an area of 104 km² and
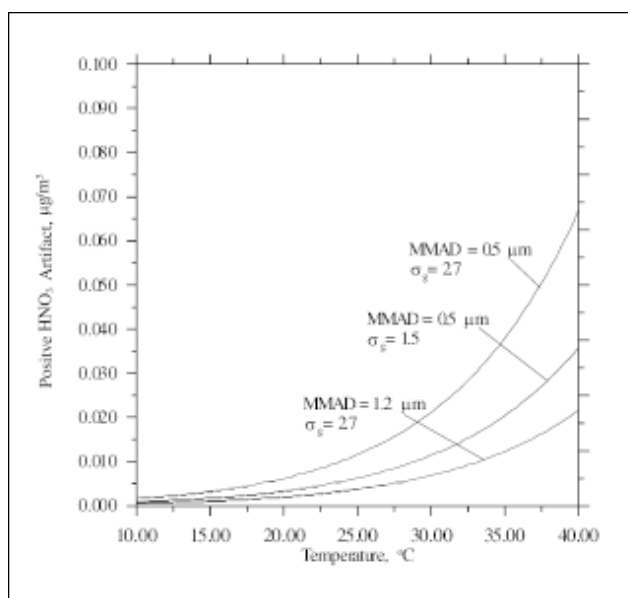
a population of nearly 340,000. This typical urban city is crowded with cars and is renowned for its high-tech semiconductor and computer industries. It is located in the northern part of Taiwan, near Taiwan's western coast.

An ADS, an HDS, and a MOUDI (MSP model 100) were used to collect acidic aerosols. While there were 15 ADS and HDS samples, there were only 10 successful MOUDI samples collected. The ambient temperature and humidity were measured by a Q-Trak (model 8550/8551, TSI). The components of the HDS include an impactor with the 50% cut size at 2.5 µm, a glass-transition section, two honeycomb denuders, a spacer, and a filter pack.[4,5] The flow rate of the HDS is 10 L/min. The first denuder was coated with $Na_2CO_3$/glycerol to collect acidic gases, such as $SO_2$, $HNO_3$, and $HNO_2$, whereas the second denuder was coated with 2% citric acid/1% glycerol in water:methanol solution to collect basic gases such as $NH_3$. A three-stage filter pack was placed downstream of the denuders. The filter pack consists of a Teflon filter (Gelman Science, 2-µm pore size) to collect fine particles, a nylon filter (Gelman Science, 1-µm pore size) to collect $HNO_3$ and HCl, and a glass fiber filter (AP40, Millipore Inc.) coated with citric acid to collect $NH_3$ that volatilized from the collected particles on the Teflon filter. Particulate $NO_3^-$ and $Cl^-$ concentrations were determined as the sum of those collected on the Teflon filter and the nylon filter, respectively.

Details of the ADS sampler were described by the U.S. Environmental Protection Agency (EPA).[13] The ADS consists of a 2.5-µm cut-size cyclone (10 L/min flow rate, model URG-2000-30EN) to remove fine particles and four

denuders to collect acidic and basic gas species. As in the case of HDS, following the fourth denuder is a PTFE Teflon filter pack, containing a Teflon filter upstream of two nylon filters (to collect $HNO_3$ and HCl) and a citric-acid-coated glass fiber filter (to collect $NH_3$). Both nylon filters were analyzed for $NO_3^-$ and $Cl^-$ concentrations.

The size distributions of airborne aerosols were measured using the MOUDI. At the entrance of the MOUDI, air first passed through two citric-acid-coated denuders, which protected the collected acidic aerosol sample from being neutralized. The MOUDI has a high flow rate of 30 L/min. The impaction substrates and final filter are Teflon filters (Gelman Science, 2-μm pore size) chosen for low background species concentrations.

After sampling, the denuders and the glass fiber filters were extracted with 10 mL of ultrapure water (Millipore, Millie-Q water system). The nylon filters were extracted with 10 mL of anion eluent (1.8 mM $Na_2CO_3$ and 1.7 mM $NaHCO_3$) to extract $Cl^-$ and $NO_3^-$ efficiently.[13] Teflon filters were extracted with 3 mL of solution containing $10^{-4}$ N $HClO_4$ and 0.04 M KCl for pH analysis. The pH determinations were made using a pH meter. The use of a small volume of extraction solution (3 mL) resulted in a satisfactory sensitivity for our analysis.[4] Concentrations of $H^+$ were then calculated by the pH of the sample using a standard calibration curve determined from known concentrations of $H_2SO_4$. Finally, soluble ions such as $NO_3^-$, $NO_2^-$, $Cl^-$, $SO_4^{2-}$, $Na^+$, $NH_4^+$, and $K^+$ were analyzed by ion chromatography (model 4500i, Dionex Corp.) following the method described in Sioutas et al.[5] The detection limits for $H^+$, $NO_3^-$, $NO_2^-$, $Cl^-$, $SO_4^{2-}$, $Na^+$, $NH_4^+$, and $K^+$ were found to be 0.003, 0.07, 0.03, 0.04, 0.08, 0.05, 0.001, and 0.05 μg/m³, respectively, based on airborne species concentrations.

## RESULTS AND DISCUSSION
### Species Concentrations and Performance Comparison of ADS and HDS

As shown in Table 1, ratios of the positive ion to the negative ion concentrations $[(H^+ + NH_4^+ + Na^+ + K^+)/(NO_3^- + Cl^- + 2SO_4^{2-})]$ for the ADS and the HDS found on the Teflon filter average 0.96 ± 0.18 (range 0.65–1.33) and 1.01 ± 0.14 (range 0.75–1.25), respectively. The ratios are all near 1.0, suggesting that all anions associated with acidity have been accounted for and these ionic species are the major composition of ionic species in the fine mode.

Molar ratios of $H^+/SO_4^{2-}$ equal to 0.0, 0.5, 1.0, and 2.0 correspond to compositions of $(NH_4)_2SO_4$, $NH_4HSO_4^-$, $(NH_3)_3H(SO_4)_2$ and $H_2SO_4$.[4] The molar ratios of $H^+/SO_4^{2-}$ measured by the ADS and HDS range from 0.08 to 1.68 (0.36 average) and from 0.05 to 1.64 (0.42 average), respectively, as shown in Table 1. Hence, acidic aerosols exist as a form distributed between $(NH_4)_2SO_4$, $(NH_3)_3H(SO_4)_2$, and $NH_4HSO_4^-$ [mainly $(NH_4)_2SO_4$ and $(NH_3)_3H(SO_4)_2$].

**Table 1.** The molar ratio of gaseous and particulate species for ADS and HDS.

| | Mean Molar Ratio ± SD, nmol/nmol | |
|---|---|---|
| | ADS Avg. ± SD (Range) | HDS Avg. ± SD (Range) |
| $H^+/SO_4^{2-}$ | 0.36 ± 0.41 (0.08 ~ 1.68) | 0.42 ± 0.54 (0.05 ~ 1.64) |
| $NH_4^+/SO_4^{2-}$ | 4.82 ± 3.92 (1.75 ~ 14.25) | 4.93 ± 3.75 (2.04 ~ 14.85) |
| $(NH_4^+ + H^+ + K^+ + Na^+)/(2SO_4^{2-} + NO_3^- + Cl^-)$ | 0.96 ± 0.18 (0.65 ~ 1.33) | 1.0 ± 0.14 (0.75 ~ 1.25) |

This study has also used the thermodynamic principle to calculate the theoretical $NH_4NO_3$ dissociation constant, which is then compared with the experimental data. Analysis of the experimental data supports that particulate $NH_4NO_3$ is in equilibrium with its precursors, $NH_3$ and $HNO_3$, in the atmosphere. The ionic species and gas-phase concentrations are shown in Table 2. On average, the concentrations (in μg/m³) of major ionic species measured by ADS are 0.019 (average) ± 0.01 [standard deviation (SD)], 7.60 ± 5.08, 7.6 ± 5.50 and 5.27 ± 2.90 for $H^+$, $SO_4^{2-}$, $NO_3^-$, and $NH_4^+$, respectively. The major gas-phase concentrations

**Table 2.** Comparison of species concentrations and mean concentration ratios (ADS/HDS).

| Species | Avg. Concentration ± SD, μg/m³ (Range) | | Avg. Concentration Ratio ± SD |
|---|---|---|---|
| | ADS | HDS | ADS/HDS |
| $HNO_3$ | 0.44 ± 0.22 (0.13 ~ 1.06) | 0.74 ± 0.30 (0.21 ~ 1.50) | 0.52 ± 0.13 |
| $HNO_2$ | 3.28 ± 2.61 (0.00 ~ 8.69) | 3.61 ± 3.10 (0.00 ~ 10.65) | 0.96 ± 0.27 |
| $SO_2$ | 23.31 ± 4.35 (5.81 ~ 63.48) | 26.92 ± 17.27 (6.79 ~ 71.05) | 0.89 ± 0.20 |
| $NH_3$ | 12.75 ± 6.65 (7.00 ~ 30.56) | 12.35 ± 4.99 (6.40 ~ 27.56) | 1.03 ± 0.24 |
| $Cl^-$ | 2.13 ± 2.63 (0.11 ~ 7.85) | 1.86 ± 2.07 (0.09 ~ 8.08) | 1.14 ± 0.25 |
| $NO_3^-$ | 7.67 ± 5.50 (1.18 ~ 21.58) | 6.80 ± 6.50 (1.05 ~ 17.78) | 1.12 ± 0.16 |
| $SO_4^{2-}$ | 7.60 ± 5.08 (1.37 ~ 16.54) | 7.61 ± 5.26 (1.11 ~ 18.37) | 1.05 ± 0.17 |
| $NH_4^+$ | 5.27 ± 2.90 (1.14 ~ 9.42) | 5.34 ± 3.12 (1.01 ~ 10.58) | 1.08 ± 0.12 |
| $Na^+$ | 1.30 ± 1.11 (0.00 ~ 4.12) | 1.36 ± 1.14 (0.00 ~ 3.91) | 0.94 ± 0.19 |
| $K^+$ | 0.75 ± 0.31 (0.00 ~ 4.46) | 0.75 ± 1.40 (0.00 ~ 4.96) | 0.91 ± 0.13 |
| $H^+$ | 0.019 ± 0.01 (0.00 ~ 0.34) | 0.019 ± 0.01 (0.00 ~ 0.046) | 1.11 ± 0.54 |

in $\mu g/m^3$ measured by the ADS are $0.44 \pm 0.22$, $3.28 \pm 2.61$, $23.31 \pm 14.35$, and $12.75 \pm 6.65$, for $HNO_3$, $HNO_2$, $SO_2$, and $NH_3$, respectively. The mean $H^+$ concentration is equivalent to $18.98$ $nmol/m^3$. In Figure 4, the concentration of $H^+$ measured by both denuder samplers is shown in the bottom panel, while the ambient condition is shown in the top panel. The first four data points were collected in the winter season, while the other points were collected in the spring season. Good correlation between the measured values by the two denuder samplers can be seen. In addition, aerosol acidity is seen not to depend on ambient temperature and relative humidity.

Comparison of major gas and particle species concentrations between the two denuder samplers is shown in Figures 5a–5f. It can be seen that the correlation between the concentrations measured by the two denuder samplers is generally very good. The difference between the concentrations measured by the ADS and the HDS for

particulate $SO_4^{2-}$, $NH_4^+$, $H^+$, $K^+$, $Na^+$, and gas-phase $NH_3$ is within $\pm 15\%$. However, the $HNO_3$ concentration measured by the ADS is consistently lower than that measured by the HDS. Both the HDS and the ADS have a similar aerosol retention time of $0.15$ sec, and previous theoretical analysis showed that positive $HNO_3$ artifact resulting from evaporation of $NH_4NO_3$ is negligibly small for both samplers. Therefore, there must be causes other than positive $HNO_3$ artifact formation. Sioutas et al.[5] found that $HNO_3$ loss in the improved HDS is smaller than that in the original HDS, since the impactor surface of the former is much smaller than that of the latter. The cyclone used by the ADS has a much larger surface area than that of the impactor used by the HDS and could also possibly result in a higher $HNO_3$ loss in the ADS.

The filter pack in the ADS has two nylon filters, while the HDS has only one nylon filter to absorb HCl and $HNO_3$ volatilized from the Teflon filter. As shown
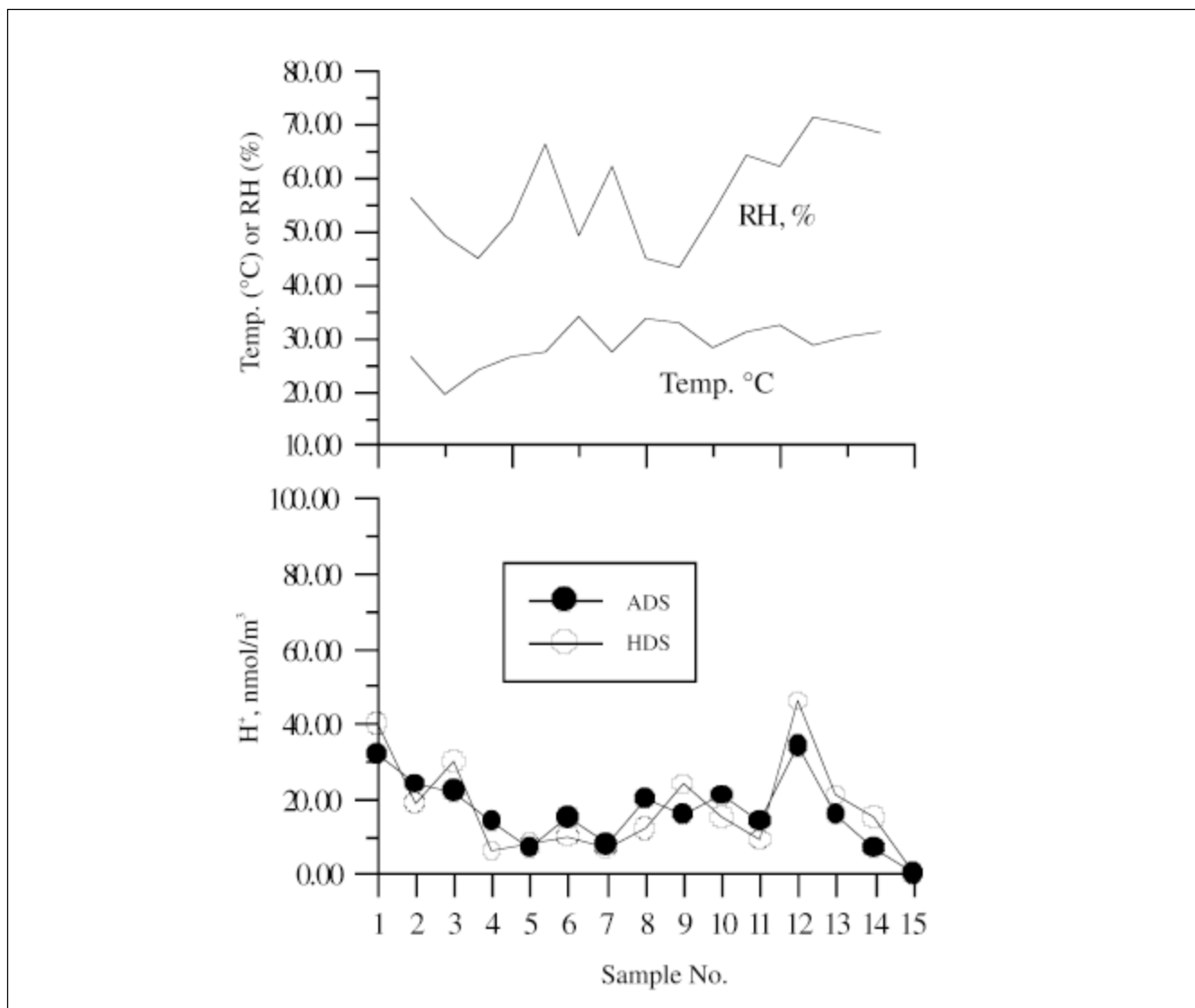


**Figure 4.** $H^+$ concentration measured by the two denuder samplers (bottom panel) and ambient condition (top panel).
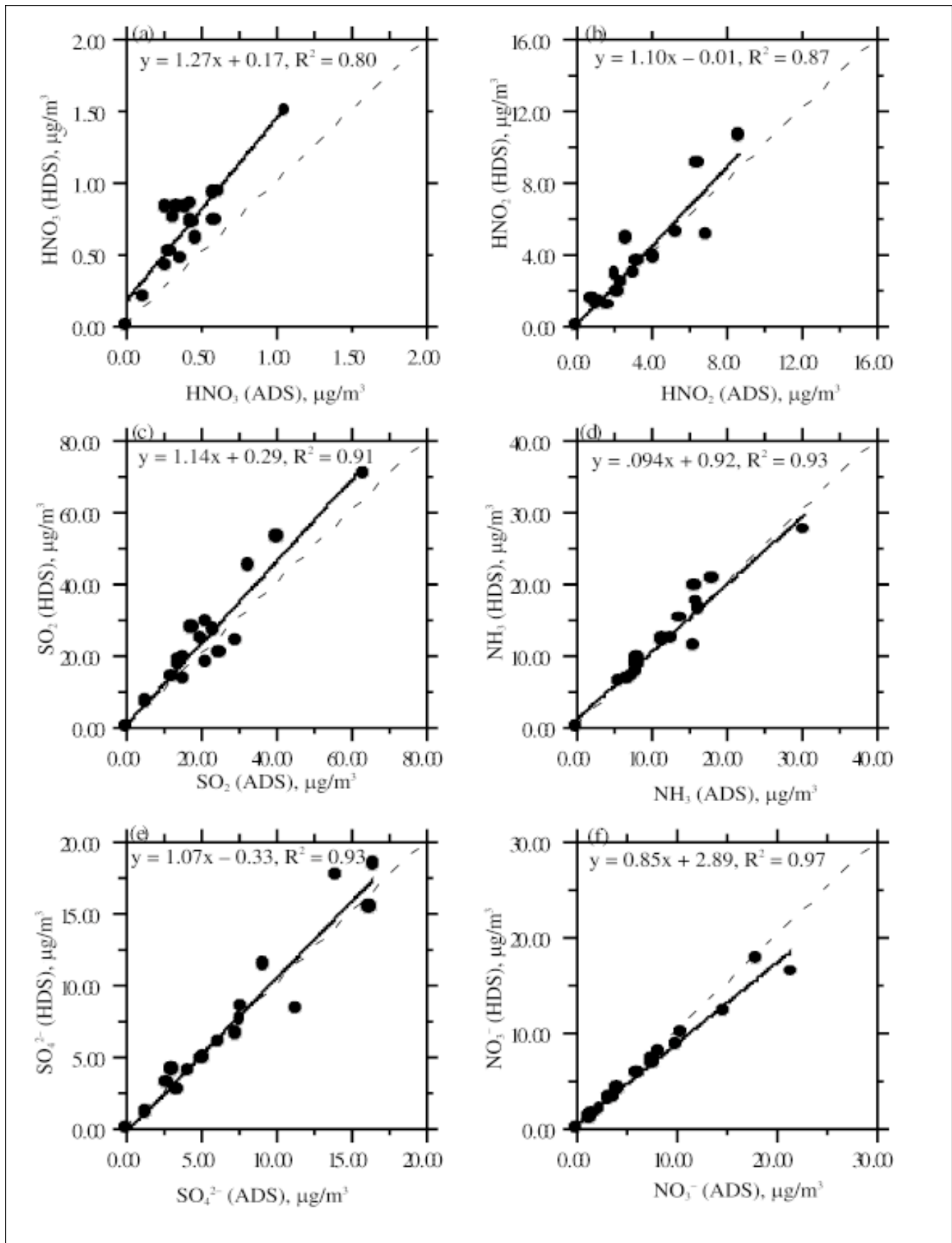
**Figure 5.** Comparison of concentrations of major gas and particle species measured by the two denuder samplers (conversion factor for gas species: 1 ppb = 2.58 μg/m³ for $HNO_3$, 1.92 μg/m³ for $HNO_2$, 2.62 μg/m³ for $SO_2$, and 0.695 μg/m³ for $NH_3$, at 1 atm and 20 °C).

**Table 3.** The concentration ratio of NF2/ADS for particulate $Cl^-$ and $NO_3^-$.

| Sample | Concentration Measured by ADS, $\mu g/m^3$ | | Concentration Measured by the NF2 in ADS, $\mu g/m^3$ | | Ratio of NF2/ADS | |
|---|---|---|---|---|---|---|
| | $Cl^-$ | $NO_3^-$ | $Cl^-$ | $NO_3^-$ | $Cl^-$ | $NO_3^-$ |
| 1 | 1.11 | 7.69 | 0.28 | 1.15 | 0.25 | 0.15 |
| 2 | 4.96 | 1.18 | 0.55 | 0.19 | 0.11 | 0.16 |
| 3 | 6.91 | 6.11 | 0.63 | 0.79 | 0.09 | 0.13 |
| 4 | 7.85 | 8.37 | 1.10 | 1.00 | 0.14 | 0.12 |
| 5 | 0.21 | 9.99 | 0.02 | 1.10 | 0.07 | 0.11 |
| 6 | 0.54 | 1.37 | 1.08 | 0.19 | 0.07 | 0.14 |
| 7 | 0.41 | 3.90 | 0.07 | 0.66 | 0.13 | 0.17 |
| 8 | 0.59 | 17.93 | 0.10 | 3.05 | 0.10 | 0.17 |
| 9 | 2.13 | 21.58 | 0.45 | 3.02 | 0.15 | 0.14 |
| 10 | 0.85 | 10.43 | 0.12 | 1.25 | 0.09 | 0.13 |
| 11 | 3.42 | 14.70 | 0.58 | 2.65 | 0.12 | 0.19 |
| 12 | 0.53 | 2.40 | 0.08 | 0.26 | 0.17 | 0.11 |
| 13 | 0.11 | 1.76 | 0.03 | 0.21 | 0.13 | 0.12 |
| 14 | 0.87 | 3.43 | 0.16 | 0.45 | 0.10 | 0.13 |
| 15 | 1.43 | 4.14 | 0.25 | 0.53 | 0.17 | 0.13 |
| Average | 2.13 | 7.67 | 0.30 | 1.10 | 0.14 | 0.14 |

in Table 3, the average concentrations of $Cl^-$ and $NO_3^-$ on the second nylon filter (NF2) of the ADS are 0.30 and 1.10 $\mu g/m^3$, respectively, which are ~14% of the total $Cl^-$ or $NO_3^-$ concentrations. That is, breakthrough of both HCl and $HNO_3$ gases from the first nylon filter has occurred. Further study of the collection efficiency and capacity of these two gases by the nylon filter is important and necessary.

### Size Distributions of Acidic Aerosols

As shown in Figures 6 and 7, $H^+$ and $NH_4^+$ were found to be in the single mode in the atmosphere, and the average MMADs are 0.63 and 0.4 ~ 0.5 $\mu m$, respectively. The size distribution of $NO_3^-$ is usually found to be bimodal. A typical distribution is shown in Figure 8. There is a fine mode for size distributions of $NO_3^-$, and the MMAD is from 0.5 ~ 1.2 $\mu m$. Fine $NO_3^-$ is usually the result of the $HNO_3/NH_3$ reaction for the formation of particulate $NH_4NO_3$, while coarse $NO_3^-$ is the product of coarse particles/$HNO_3$ reactions.

The size distribution of $SO_4^{2-}$ is usually found to be bimodal, as shown in Figure 9 for a typical distribution. There are two submicron modes for size distributions of $SO_4^{2-}$. The two modes are called the condensation mode, with an MMAD of 0.18 ~ 0.32 $\mu m$, and the droplet mode, at 0.92 ~ 1.04 $\mu m$. However, there is only one supermicron mode for $SO_4^{2-}$, and the average diameters are 7.00 ~ 7.95 mm.

The ratios of $SO_4^{2-}$, $NO_3^-$, $NH_4^+$, $H^+$, $Cl^-$, $Na^+$, and $K^+$ in fine particles are $74 \pm 20\%$, $71 \pm 10\%$, $96 \pm 5\%$, $98 \pm 1\%$, $60 \pm$ 5%, $51 \pm 14\%$, and $58 \pm 16\%$, respectively, as shown in Table 4. It indicates that $SO_4^{2-}$, $NO_3^-$, $NH_4^+$, and $H^+$ are dominant in the fine fraction of particles, whereas $Cl^-$, $Na^+$, and $K^+$ are found in both fine and coarse particles. One can also see in Table 4 that total anion (2 $[SO_4^{2-}]$ + $[NO_3^-]$ + $[Cl^-]$) and cation ($[H^+]$ + $[NH_4^+]$ + $[Na^+]$ + $[K^+]$) nanoequivalents are nearly the same (326.67 vs. 323.86 $nmol/m^3$) for fine particles, while that is not the case for coarse particles (225.29 vs. 77.7 $nmol/m^3$). This suggests that neutralization by alkaline species other than $Na^+$ and $K^+$ has occurred for coarse particles, but probably not for fine particles. Whether or not alkaline species other than $Na^+$ and $K^+$ appear in significant amounts in fine particles involves further chemical analysis of fine particle samples by atomic absorption spectrometry, but this is beyond the scope of the present work.

### CONCLUSIONS

The acidic aerosols and the particle size distributions were measured with the ADS, HDS, and MOUDI simultaneously in Hsinchu. The samples were analyzed by ion chromatography for ionic and gas species concentrations. Theoretical analysis of the problem of positive $HNO_3$ artifact due to evaporation loss of $NO_3^-$ particles can be neglected for both denuder samplers. If the ambient temperature is below 28 °C, the maximum $HNO_3$ artifact concentration is less than 0.01 $\mu g/m^3$ when the maximum $NO_3^-$ concentration is 17.9 $\mu g/m^3$.

Experimental results conclude that the HDS performs equally as well as the ADS for atmospheric aerosol

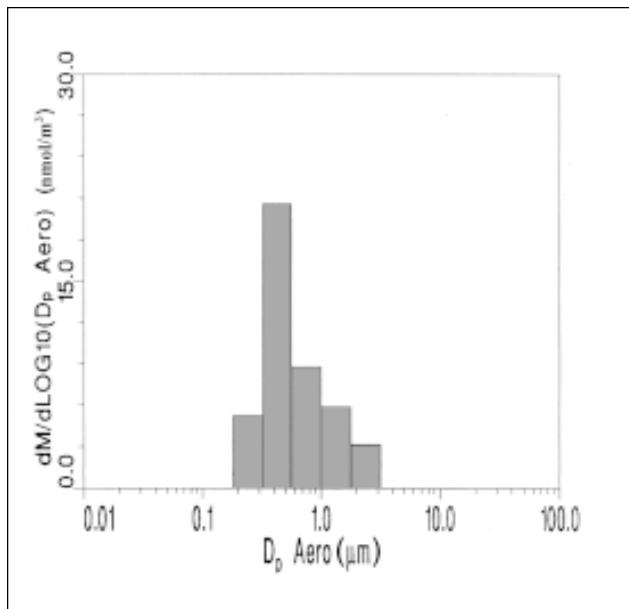**Figure 6.** A typical H+ size distribution (single mode). The *x* axis refers to particle aerodynamic diameter.



**Figure 8.** A typical $NO_3^-$ size distribution (bimodal). The *x* axis refers to particle aerodynamic diameter.

sampling, except for the measurement of the gas-phase $HNO_3$. For $HNO_3$, the concentrations measured by the HDS are consistently higher than those measured by the ADS, possibly because there is a higher $HNO_3$ loss in the cyclone used by the ADS than in the impactor used by the HDS. About 14% of the total $Cl^-$ and $NO_3^-$ were measured in the second nylon filter of the filter pack of the ADS, suggesting that breakthrough of HCl and $HNO_3$ from the first nylon filter is occurring. Further study of the collection efficiency and capacity of HCl and $HNO_3$ gases by the nylon filter is warranted. In this study, $SO_4^{2-}$, $NO_3^-$,
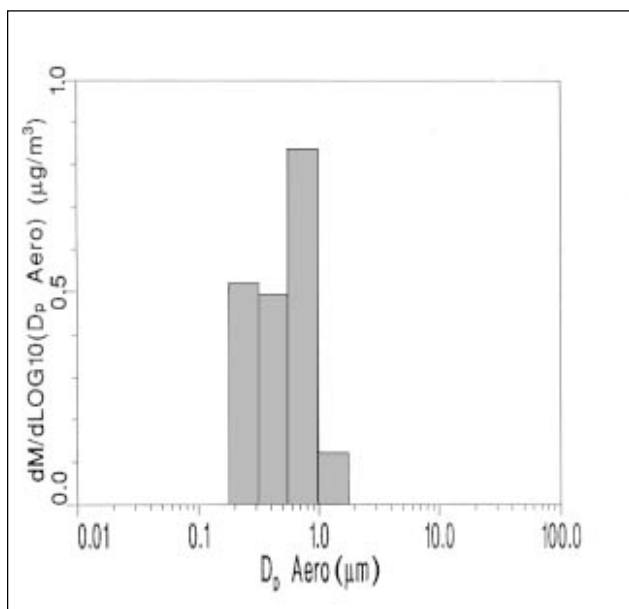
$NH_4^+$, and H+ were found to be dominant in the fine fraction of particles, whereas $Cl^-$, $Na^+$, and $K^+$ were found in both fine and coarse particles. $NH_4^+$ and H+ have a single fine particle mode, while $SO_4^{2-}$ and $NO_3^-$ usually have both fine and coarse particle modes.

**ACKNOWLEDGMENT**

**Figure 7.** A typical $NH_4^+$ size distribution (single mode). The *x* axis refers to particle aerodynamic diameter.
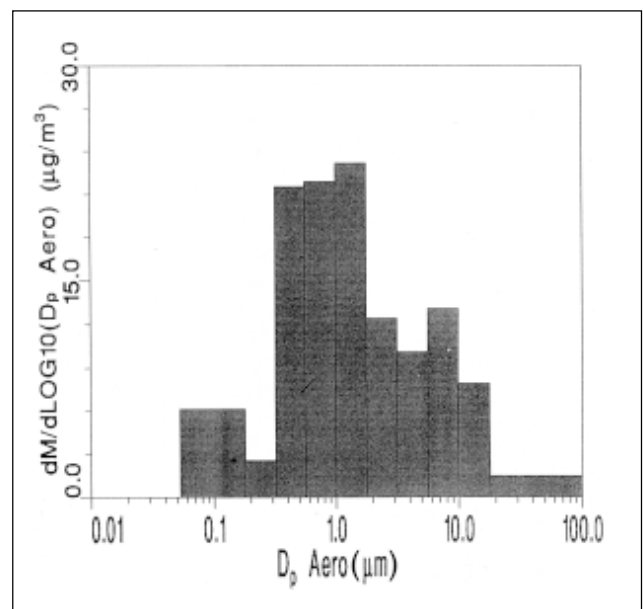


**Figure 9.** A typical $SO_4^{2-}$ size distribution (bimodal). The *x* axis refers to particle aerodynamic diameter.

**Table 4.** The ratio of soluble ions in particles collected by the MOUDI.

| Species | Number of Tests | Avg. Concentration in Fine Particles ± SD, nmol/m³ | Avg. Concentration in Coarse Particles ± SD, nmol/m³ | Ratio of Soluble Ions in Fine Particles ± SD, % |
|---|---|---|---|---|
| $SO_4^{2-}$ | 10 | 92.68 ± 66.99 | 56.45 ± 48.76 | 74 ± 20 |
| $NO_3^-$ | 10 | 108.19 ± 95.66 | 78.18 ± 73.26 | 71 ± 10 |
| $Cl^-$ | 10 | 33.12 ± 28.04 | 34.2 1 ± 28.80 | 60 ± 5 |
| $NH_4^+$ | 10 | 214.37 ± 164.59 | 6.32 ± 14.41 | 96 ± 5 |
| $H^+$ | 10 | 13.84 ± 6.27 | 0.02 ± 0.07 | 98 ± 1 |
| $Na^+$ | 10 | 65.38 ± 45.20 | 54.15 ± 29.75 | 51 ± 14 |
| $K^+$ | 10 | 30.27 ± 40.60 | 17.23 ± 18.63 | 58 ± 16 |
| Total anion nanoequivalents | | 326.67 ± 257.68 | 225.29 ± 199.58 | |
| Total cation nanoequivalents | | 323.86 ± 256.66 | 77.7 ± 45.86 | |

## REFERENCES

1. Spengler, J.D.; Brauer, M.; Koutrakis, P. Acid Air and Health; *Environ. Sci. Technol.* **1990**, *24*, 946.
2. Koutrakis, P.; Wolfsan, M.; Spengler, J.D. An Improved Method for Measuring Aerosol Strong Acidity: Result from a Nine-Month Study in St. Louis, Missouri, and Kingston, Tennessee; *Atmos. Environ.* **1988**, *22*, 157.
3. Possanzini, M.; Febo, A.; Liberti, A. New Design of a High-Performance Denuder for the Sampling of Atmospheric Pollutants; *Atmos. Environ.* **1983**, *17*, 2605.
4. Koutrakis, P.; Sioutas, C.; Ferguson, S.T.; Wolfsan, J.M. Development and Evaluation of a Glass Honeycomb Denuder/Filter Pack System To Collect Atmospheric Gases and Particles; *Environ. Sci. Technol.* **1993**, *27*, 2497.
5. Sioutas, C.; Wang, P.Y.; Ferguson, S.T.; Koutrakis, P. Laboratory and Field Evaluation of an Improved Glass Honeycomb Denuder/Filter Pack Sampler; *Atmos. Environ.* **1996**, *30*, 885.
6. Bai, H.; Lu, C.S.; Ling, Y.M. A Theoretical Study of the Evaporation of Dry Ammonium Chloride and Ammonium Nitrate Aerosols; *Atmos. Environ.* **1995**, *29*, 313.
7. Hinds, W.C. *Aerosol Technology*, 2nd ed.; Wiley: New York, 1999; Chapter 7, pp 165-168.
8. Winiwater, W. A Calculation Procedure for the Determination of the Collection Efficiency in Annular Denuders; *Atmos. Environ.* **1989**, *23*, 1997.
9. Seinfeld, J.H.; Pandis, S.N. *Atmospheric Chemistry and Physics*; Wiley: New York, 1998; Chapter 11, pp 596-607.
10. Stelson, A.W.; Seinfeld, J.H. Relative Humidity and Temperature Dependence of the Ammonium Nitrate Dissociation Constant; *Atmos. Environ.* **1982**, *16*, 983.
11. Mozurkewich, M. The Dissociation Constant of Ammonium Nitrate and Its Dependence on Temperature, Relative Humidity and Particle Size; *Atmos. Environ.* **1993**, *27*, 261.
12. Cheng, Y.H.; Tsai, C.J. Evaporation Loss of Ammonium Nitrate Particles during Filter Sampling; *J. Aerosol Sci.* **1997**, *28*, 1553.
13. *Determination of the Strong Acidity of Atmospheric Fine Particles (<2.5 mm) Using Annular Denuder Technology*; EPA/600/R-93/037; U.S. Environmental Protection Agency, U.S. Government Printing Office: Washington, DC, 1992.

**About the Authors**

Dr. Chuen-Jinn Tsai (cjtsai@green.ev.nctu.edu.tw) is a professor and Shie-Bong Perng and Shin-Fu Chiou are graduate students at the Institute of Environmental Engineering, National Chiao Tung University, No. 75, Poai St., 300 Hsinchu, Taiwan.